Frequency-modulated continuous-wave lidar using I/Q modulator for simplified heterodyne detection

S. Gao[1,2] and R. Hui[1,*]

[1]*Department of Electrical Engineering and Computer Science, University of Kansas, Lawrence, Kansas 66045 USA*

[2]*Department of Electronic Engineering and Information Science, University of Science and Technology of China, Hefei, Anhui, 230027, China*

**Corresponding author: rhui@ku.edu*

Received February 22, 2012; accepted April 4, 2012;
posted April 10, 2012 (Doc. ID 163479); published May 30, 2012

A frequency-modulated continuous-wave (FMCW) lidar is demonstrated with heterodyne detection. The lidar transmitter utilizes an electro-optic I/Q modulator for the first time to generate carrier-suppressed and frequency-shifted FM modulation. This eliminates the need for an acousto-optic frequency shifter commonly used in heterodyne lidar transmitters. It also allows the use of a much wider modulation bandwidth to improve the range resolution. The capability of complex optical field modulation of the I/Q modulator provides an additional degree of freedom compared with an intensity modulator, which will benefit future lidar applications.

OCIS codes: 060.2300, 280.3640, 120.4640.

Lidar systems have been widely used for measuring range, velocity, vibration, and air turbulence [1–3]. Coherent detection has become a major detection mechanism in lidar systems because of the much improved receiver sensitivity compared with direct detection. While homodyne detection is susceptible to the phase noise of the optical carrier and the associated signal fading, heterodyne detection is a more robust detection scheme for many practical lidar systems [4,5]. In a heterodyne receiver, mixing between the optical signal and the local oscillator (LO) shifts the optical signal to an intermediate frequency f_{IF}. In practical implementation of a lidar system, the signal and the LO are usually split from the same laser. While the signal is modulated by an electro-optic modulator, the LO has to go through an acousto-optic modulator (AOM) to create the required frequency shift f_{IF}. In addition to the increased complexity, the frequency shift of an AOM is usually not more than 1 GHz. Although the bandwidth of a practical electro-optic modulator can be higher than 40 GHz, to avoid spectral aliasing, the usable modulation bandwidth of a heterodyne detection lidar is limited by the IF frequency, which is determined by the AOM. In recent years, the rapid advance in coherent fiber-optic communication has created high-speed electro-optic in-phase/quadrature (I/Q) modulators, which are capable of modulating the amplitude and the phase of the optical carrier independently. Despite the popular application of I/Q modulators in optical communication systems, their application in lidar has not been reported.

In this paper, we demonstrate a frequency-modulated continuous-wave (FMCW) lidar system using heterodyne detection. An I/Q modulator is used to simultaneously generate the linear FM chirp required for pulse compression and the IF frequency shift required for heterodyne detection. Therefore, the optical frequency of the LO does not have to be shifted, and the AOM is not required. Based on a commercial transmitter originally designed for a 10 Gb/s optical communication system, the lidar system allows unprecedented chirping bandwidth to ensure the fine range resolution, while the optical system configuration is simplified.

For an FMCW lidar system [6], a linear frequency chirp is applied across each optical pulse. The range resolution R_{res} is determined by the chirping bandwidth, while the signal-to-noise ratio (SNR) is determined by the integrated pulse energy through pulse compression. In the lidar transmitter, intensity modulation is applied on the optical signal, and its frequency linearly increases from f_1 to f_2 within each optical pulse of duration T. For range measurement, the signal deflected from the target has a round-trip time delay Δt, which corresponds to a constant frequency shift f_{R}. This frequency shift can be measured, which is related to the range R by [7]

$$f_R = (f_2 - f_1)\Delta t/T = 2BR/(cT), \tag{1}$$

where $B = f_2 - f_1$ is the chirping bandwidth and c is the speed of light. While the range resolution $R_{\mathrm{res}} = c/(2B)$ depends only on the chirping bandwidth, the range accuracy is determined by both B and SNR, as $\sigma_R = Kc/(B\sqrt{\mathrm{SNR}})$ where K is a proportionality factor depending on the chirp waveform [8].

Figure 1 shows the block diagram of the proposed lidar system with coherent heterodyne detection. In this system, the CW source laser is split into two parts: One is used as the LO, and the other is modulated through an electro-optic I/Q modulator. The RF chirp waveform from a synthesizer is split into the I and the Q components and fed to the I/Q modulator. By properly setting

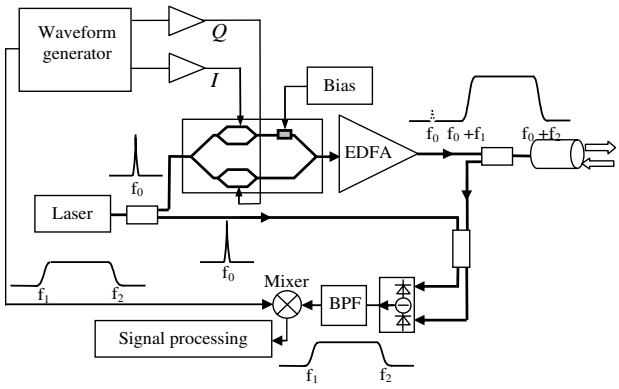

Fig. 1. Block diagram of the simplified heterodyne detection lidar system based on an I/Q modulator.

the DC bias of the modulator, the optical carrier can be suppressed, and the chirp signal can be loaded onto either the upper or the lower optical sideband. The center of the sideband is equivalent to an IF frequency $f_{\mathrm{IF}} = (f_1 + f_2)/2$ Then the single sideband optical signal is amplified by an EDFA before sending to the telescope.

In the receiver, the backscattered optical signal from the target is combined with the LO in an optical coupler and detected by a balanced photodiode. The heterodyne RF spectrum centralized at f_{IF} is selected by an RF bandpass filter (BPF) and then mixed with the original chirp waveform to find the differential frequency f_R through signal processing so that the target range can be determined.

As illustrated in Fig. 1, an I/Q modulator consists of two Mach—Zehnder (MZ) intensity modulators, one on each arm of a MZ interferometer, with a DC phase shifter between the two arms. For FMCW lidar operation, the two voltage waveforms used to drive the I and Q arms of the modulator within each optical pulse ($0 \le t \le T$) are

$$V_I(t) = V_D \cos\left(2\pi f_1 t + \pi \frac{f_2 - f_1}{T} t^2\right), \tag{2}$$

$$V_Q(t) = V_D \sin\left(2\pi f_1 t + \pi \frac{f_2 - f_1}{T} t^2\right), \tag{3}$$

where V_D is the amplitude of the driving voltage signal. Assume the optical frequency of the CW laser is f_0, the intensity modulators of I and Q branches are both biased at the null point, and the phase shifter is biased at the quadrature point, the optical field at the modulator output is [9]

$$E_0 = E_s\left[\sin\left(\frac{\pi V_I(t)}{V_\pi}\right)\cos(2\pi f_0 t) + \sin\left(\frac{\pi V_Q(t)}{V_\pi}\right)\sin(2\pi f_0 t)\right], \tag{4}$$

where E_s is the constant input optical field and V_π is the voltage required for the transfer function to change from the minimum to the maximum for each intensity modulator. Equation (4) can be linearized when $V_D/V_\pi \ll \pi$, so that

$$E_0 \approx E_s \cos\left[2\pi f_0 t - \left(2\pi f_1 t + \pi \frac{f_2 - f_1}{T} t^2\right)\right]. \tag{5}$$

This is a carrier-suppressed single-sideband optical signal with the central frequency shift $f_{\mathrm{IF}} = (f_2 + f_1)/2$ from the optical carrier frequency f_0. In general, either the upper or the lower optical sideband can be generated by setting the phase shift at $+\pi/2$ or $-\pi/2$.In our experiment, the lidar transmitter is built based on a Ciena commercial optical transmitter originally designed for 10 Gb/s optical transmission with electronic domain precompensation (eDCO) [9]. This transmitter is equipped with two 21.42 GS/s digital-to-analog converters (DAC) with 6-bit resolution. An on-board digital memory is available with 2^{15} bits in length so that the maximum period of the arbitrary waveform that can be generated by this transmitter is 1.5298 μs. The I/Q modulator used in the system has 10 GHz modulation bandwidth. To fit for coherent detection, we have used a tunable laser with a 100 kHz linewidth (Agilent 81642A) as the light source, and the wavelength was set at 1549.54 nm in the experiment. The chirp signal is digitally generated and loaded to the onboard memory. The digital waveforms are converted to analog format through the DACs to drive the I/Q modulator after RF amplification.

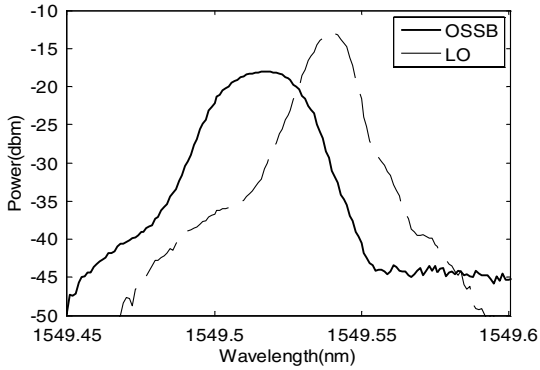

Fig. 2. Optical single sideband modulated signal and optical LO.

At the receiver, the optical signal reflected from the target is mixed with the LO at a photodiode with 30 GHz bandwidth. In order to investigate the optical and the RF down-conversion processes, a real-time oscilloscope (LeCory 8600A) with a 20 Gs/s sampling rate is used immediately after the RF pre-amplifier, so that the IF signal after heterodyne detection can be digitally recorded and processed. Because the major purpose of this work is to demonstrate the heterodyne system using I/Q modulator, we used a 20 m fiber delay line in place of the telescope in the experiment to avoid the complication due to free-space optical coupling and the associated power and range uncertainty.

Figure 2 shows an example of the optical spectra measured by an optical spectrum analyzer (OSA) with

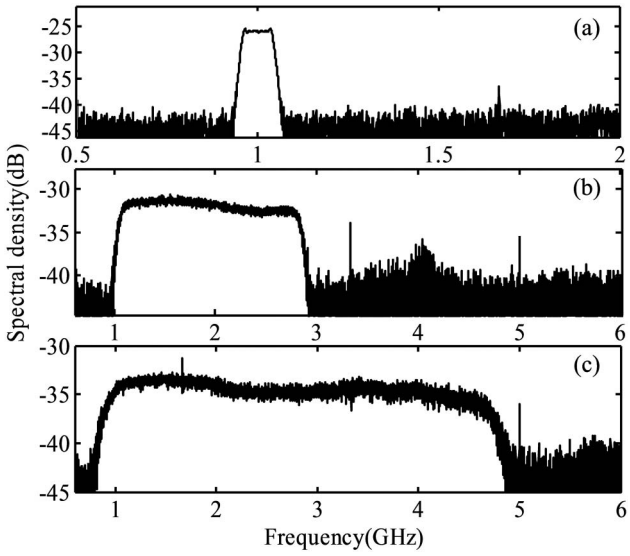

Fig. 3. Heterodyne IF spectra with $B = 100$ MHz (a), $B = 2$ GHz (b), and $B = 4.3$ GHz (c).

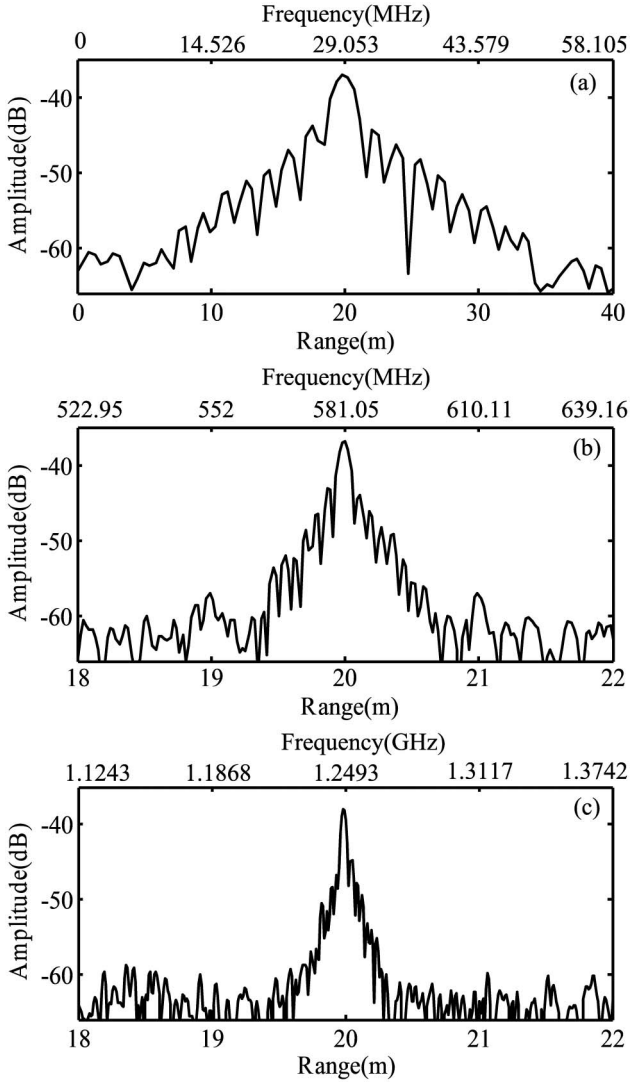

Fig. 4. Frequency down-converted spectra for the system with 100 MHz (a), 2 GHz (b), and 4.3 GHz (c) modulation bandwidths.

0.01 nm resolution, which includes the LO and the carrier-suppressed single-sideband optical signal with a 4 GHz chirp bandwidth at $f_{\mathrm{IF}} = 3$ GHz. The power suppression ratio of the opposite modulation sideband is >25 db. Figure 3 shows the received heterodyne IF spectra recorded by the real-time oscilloscope for three different chirping bandwidths of 100 MHz, 2 GHz, and 4.3 GHz, respectively. A raised cosine window function was applied to the chirping signal to minimize the edge effect. In the time domain, the pulse repetition rate is 1.5298 μs, determined by the length of the digital memory, and the pulse width of the optical signal is chosen as $T = 0.6884$ μs in the experiment.

In order to obtain the target range information, the recorded IF signal is bandpass filtered and digitally mixed with the original chirp waveform for frequency down-conversion. Figure 4 shows the spectra of the down-converted signals corresponding to three different chirping bandwidths of the optical signal. The top and bottom horizontal axes indicate the frequency and the corresponding target range, respectively, calculated from Eq. (1). Although all three measurements predict the same length of 20 m for the fiber delay line, their spectral widths are different, which represent the range resolution.

The 3 dB spectral widths in Figs. 4(a), 4(b), and 4(c) indicate the range resolutions of 89 cm, 4.7 cm, and 2.3 cm, corresponding to the chirping bandwidths of 100 MHz, 2 GHz, and 4.3 GHz, respectively. For all three measurements shown in Fig. 4, a relatively high signal optical power (approximately −20 dBm) was used to ensure sufficiently high SNR so that the range resolution can be accurately measured.

In conclusion, we have demonstrated a simplified coherent heterodyne lidar system using an electro-optic I/Q odulator. Carrier-suppressed single-sideband modulation eliminated the need for an AOM for carrier frequency shift. It also allowed full utilization of modulator bandwidth to achieve fine range resolution. The ability of complex optical field modulation provided an additional degree of freedom, which can be used in both FMCW and short-pulse lidar systems. Although our measurements were conducted in a fiber delay line setup, the operation principle can be readily extended to free-space applications such as lidar velocity measurements with direction discrimination.

This work was supported in part by Ciena Corp, and by KU Transportation Research Institute (TRI). The authors would like to thank Dr. M. O'Sullivan and Dr. C. Allen for many helpful discussions. S. Gao acknowledges the financial support from China Scholarship Council (CSC).

References

1. J. M. Vaughan, Physica Scripta **T78**, 73 (1998).
2. C. J. Karlsson, F. A. A. Olsson, D. Letalick, and M. Harris, Appl. Opt. **39**, 3716 (2000).
3. M. Harris, R. I. Young, F. Kopp, A. Dolfi, and J.-P. Cariou, Aerosp. Sci. Technol. **6**, 325 (2002).
4. A. Dolfi-Bouteyre, G. Canat, M. Valla, B. Augere, C. Besson, D. Goular, L. Lombard, J.-P. Cariou, A. Durecu, D. Fleury, L. Bricteux, S. Brousmiche, S. Lugan, and B. Macq, IEEE J Sel. Top. Quant. **15**, 441 (2009).
5. M. Harris, R. I. Young, F. Köpp, A. Dolfi, and J. Cariou, Aerosp. Sci. Technol. **6**, 325 (2002).
6. C. J. Karlsson and F. A. Olsson, Appl. Opt. **38**, 3376 (1999).
7. P. Adany, C. Allen, and R. Hui, J. Lightwave Technol. **27**, 3351 (2009).
8. L. J. Mullen, A. J. C. Vieira, P. R. Herczfeld, and V. M. Contarino, IEEE T. Microw. Theory **43**, 2370 (1995).
9. Y. Zhang, M. O'Sullivan, and R. Hui, Opt. Express **19**, 21880 (2011).